

Faraday Angle and Accuracy Measurement of Magneto-Optic Current Transmission Based on New Telluride Glass

ShiYu Yin , ZhiZhi Zhang, Yong Li , Hao Wang, Lin Liu, TianJiao Zhou, and ShiFeng Wang

Abstract—Two robust temperature-insensitive magneto-optical current sensor prototypes, based on double polarimetric processing schemes and single light way methods, were constructed using light reflection and light transition, respectively. A diamagnetism $\text{TeO}_2\text{-PbO-ZnO-BaF}_2$ bulk glass was fabricated as a sensing head which, with/without a silver layer, acts as a mirror sputtered by RF sputtering. The Verdet constant of the TPZBF glass was measured using the self-made optical bench. The current sensors were evaluated under various currents and different temperatures. Results indicated that the constructed low-cost current sensor prototypes are accurate and stable for current sensing applications.

Index Terms—Faraday effect, current sensor, tellurite glass.

I. INTRODUCTION

IMPROVING the accuracy of electrical measurement is an important part of sustainable energy management system research. Current sensors can quickly identify faults in the power system and accurately measure power consumption, so they are essential tools today [1]. However, the commonly used traditional current transformers have many limitations because, in the real environment, they can be easily damaged by heat, short-circuits, or atmospheric electrical discharges. It is essential to employ protection circuits and insulation, which requires constant maintenance and surveillance. By contrast, an optical current sensor (OCT) is appealing for applications in high power systems because it has several advantages such as light

weight/small size; immunity against electromagnetic interferences; electrical isolation; and the possibility for measuring AC / DC and so on [2], [3].

There are two types of OCT (all-fiber optic sensors and bulk-optic based sensors) using the Faraday effect that were analyzed. The most easily implemented and researched sensors are all-fiber current sensors, which have relatively low Verdet constants, and have problems such as high linear birefringence and excessive bending loss. While on the contrary, most industrial implementation technologies use bulk optic sensors [4], because these kinds of sensors present almost no linear birefringence, are a smaller size, mechanically stiffer, and have more minor vibrations and external noises and higher Verdet constants; these advantages allow for the sensors' high sensitivities [5]. Despite these promising properties of OCT, they are still costly and have limited performance due to the sensing materials.

According to the principle of the Faraday effect, the basis for obtaining high sensitivity is the use of highly rotating materials. Currently used high Verdet constant materials are crystals such as YIG, which are very expensive and have easy saturation effects of high voltage. Magneto-optical glass has become a potential material for replacing crystals because of its low cost and easy processing. Among the magneto-optical glasses, the paramagnetic glass needs temperature compensation installation, which increases the price and size of this sensor. Unlike crystal and paramagnetic glass counterparts, the Faraday effect of the diamagnetism glass is not affected by temperature. In addition, the problem that the Verdet constant of pure diamagnetism glass is usually low can be improved by changing the composition and manufacturing conditions. Also, the stability and range of operation have been improved, resulting in significant advantages in sensing and monitoring applications [6], [16].

TeO_2 -based glass has high transmittance in the wavelength range from visible light to near mid-infrared, and Te^{4+} ions have high polarizability. Therefore, TeO_2 -based glass can develop high-efficiency diamagnetism magneto-optical current sensor components.

In this study, a high Verdet constant $\text{TeO}_2\text{-PbO-ZnO-BaF}_2$ (TPZBF) glass as a sensing head was designed and fabricated [7]. A low-cost, self-made, single-light-way measurement was set up, avoiding using a lock-in amplifier or uncertainties due to variations in the optical path or light fluctuation from AC methods, significantly reduce the complexity and total cost [8].

Manuscript received 8 August 2022; accepted 18 August 2022. Date of publication 23 August 2022; date of current version 22 September 2022. This work was supported in part by the Natural Science Foundation of Tibet Autonomous Region under Grant XZ202101ZR0121G, in part by the National Natural Science Foundation of China under Grant 52062045, and in part by the Central Government Funds for Local Scientific and Technological Development under Grant XZ202201YD0026C. (Corresponding author: Yong Li).

ShiYu Yin is with the School of Mechanical and Materials Engineering, North China University of Technology, Beijing 100144, China (e-mail: yinsy@ncut.edu.cn).

ZhiZhi Zhang and Lin Liu are with the School of Mechanical and Materials Engineering, North China University of Technology, Beijing 100144, China (e-mail: ncutzzz@163.com; 11189879@163.com).

Yong Li is with the College of Science, Tibet University, Lhasa 850000, China (e-mail: liyongzzu@163.com).

Hao Wang is with the School of Instrument Science and Engineering, Harbin Institute of Technology, Harbin 150001, China (e-mail: 22b901035@stu.hit.edu.cn).

TianJiao Zhou is with the Chongqing General Aviation Industry Group Company Ltd., Chongqing 401135, China (e-mail: 546960483@qq.com).

ShiFeng Wang is with the Key Laboratory of Cosmic Rays, (Tibet University), Ministry of Education Lhasa, Lhasa 850000, China (e-mail: wsf365@163.com).

Digital Object Identifier 10.1109/JPHOT.2022.3201004

Two prototypes based on light reflection and light transitions were compared on the same sensing head with/without sputtered silver layer on one side.

II. EXPERIMENTAL WORK

The Faraday rotation effect means that the rotation of the plane of polarized light is linearly proportional to the magnetic field component in the propagation direction [3]. The Faraday rotation of the azimuth angle of the output light of the optical current sensor can be quantified using different signal analysis techniques. One of the methods to detect the rotation angle is to use a polarization detection scheme, which uses two polarizers located in front of and behind the sensor [9]. The first polarizer is used to determine the initial polarization state of the light wave. The second polarizer is used to adjust the sensor sensitivity and convert the polarization rotation into a light intensity signal that can be measured by a photodetector [4].

The Faraday effect reveals that the rotation angle β of the transmission axis of polarized light is proportional to the linear integral of the magnetic field B along path L [10]. The rotation angle β can be calculated by the following (1) when the light beam circulates on the current-carrying conductor:

$$\beta = V_d x \oint_L B dl = N_l \times N_c \times N_d \times i \quad (1)$$

Where N_l is the number of passes of light around the conductor, N_c is the number of current coils turns, i is the conductor current, and V_d is the Verdet constant of the sensing material. From (1), the β may be improved by increasing V_d and dl . In this paper, the V_d was enhanced by selecting the suitable compositions of the TPZBF glass, and dl is enhanced by using a silver layer that acts as a mirror to reflect the light and double the light way in the TPZBF bulk glass. For a given system, considering that the N_l , N_c , V_d , and dl are constants, β is a function of the applied current on conductor [11].

The sensitivity of a magneto-optical sensor is defined as the ratio of the instrument's output signal to the change of the input variable [12]. For this study, the output signal is the amount of change in the output light intensity, and the input variable is the applied current that will cause the deviation of the Faraday rotation angle β . So, the sensitivity of MOCT can be finally expressed as a function of the output signal from the photodiode to the applied current or current square. For a suitable sensor, the relationship should be linear. This relationship will be introduced and evaluated in the experimental part according to the real optical setup.

The most important work was to obtain a high Verdet constant sensing head for this system. So TPZBF glass was fabricated using a melting- quenching method at 1000 °C and annealed at 250 °C for 10 hours. A detailed composition and properties related to this glass are available in reference [7]. As showed in Table I. Install the cut and optically polished glass on the optical bench, as shown in Fig. 1 for Verdet constant measurement. A He-Ne laser with an emission efficiency of 29% is used to provide a light source with a power of 1.8 mW. A NA = 0.28 × 10 microscope objective lens is used to focus the beam on a

TABLE I
THE COMPOSITIONS AND DENSITY OF GLASS SAMPLE [7]

Sample	Mole fraction (%)				Density d (g.cm ⁻³)
	TeO ₂	PbO	ZnO	BaF ₂	
TPZBF1	60	20	19	1	6.243
TPZBF3	60	20	17	3	6.267
TPZBF5	60	20	15	5	6.295
TPZBF6	60	20	14	6	6.306
TPZBF7	60	20	13	7	6.313
TPZBF9	60	20	11	9	6.327

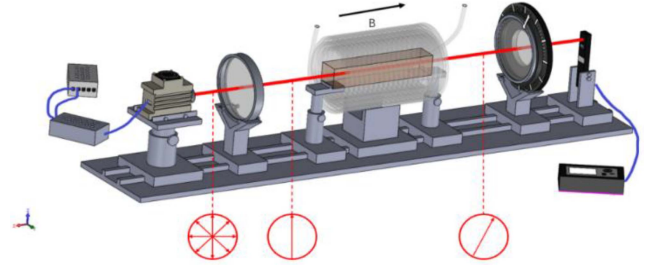


Fig. 1. Schematic diagram of Verdet constant measuring device for bulk glass.

linearly polarized laser beam with a diameter of about 1 mm. Through testing, it is found that the polarization extinction ratio of the laser beam used in this work is higher than 1:5000. The glass is surrounded by a solenoid composed of a copper wire with a diameter of 2 mm. The surrounding radius of the solenoid is $r_1 = 11.5$ mm, which is made by winding 220 turns of a PTFE tube. The total outer radius of the electric coil is $r_2 = 17$ mm. According to the Biot-Savart law, the theoretical magnetic field density of glass is distributed as shown in the following (2):

$$B_{th(x)} = \frac{\mu \cdot I \cdot N}{2l(r_2 - r_1)} \begin{bmatrix} (x + l/2) \cdot \ln \frac{\sqrt{r_2^2 + (x+l/2)^2} + r_2}{\sqrt{r_1^2 + (x+l/2)^2} + r_1} \\ -(x - l/2) \cdot \ln \frac{\sqrt{r_2^2 + (x-l/2)^2} + r_2}{\sqrt{r_1^2 + (x-l/2)^2} + r_1} \end{bmatrix} \quad (2)$$

The magnetic field density is measured at several locations using a Teslameter (PHYWE, 13610-93) and a solenoid excited by a current of 10 A [6].

The Verdet constant measurement device is shown in Fig. 1. When the device is running, the focused beam first propagates through the TPZBF glass and then passes through the analyzer installed on a rotating stage with an accuracy of 3×10^{-4} rad. The output beam's power is measured by a photodetector (Ophir PD300). The power level of the photodetector is 0.02nW, and the dynamic range is 30Db [17].

After the cut and optical polishing, the fabricated TPZBF glass (40 mm × 30 mm × 10 mm) was sent to the vacuum chamber for RF sputtering. The Ag target had a diameter of 2.54 cm. A silver layer was deposited under a vacuum pressure of 70 μPa, and RF power was 15W. The coating was homogenous and had a thickness of 20 μm.

A cheap and straightforward “unlinked” Faraday sensor for current detection using a “point measurement” in the vicinity of the conductors was employed because this design does not

require precise current measurement. When linearly polarized light passes through the sensor head in the magnetic field, it will change its plane angular. A homogeneous magnetic field was generated in the current wire. The magnetic field around a current wire can be directly modified by using a DC power supply to change the current in the wire. Therefore, the current in the transmission line can be calculated by measuring the current intensity of the photodiode. By normalizing the DC output current through the photodiode, the uncertainty associated with the change of the optical path can be easily eliminated [14].

Laboratory tests were carried out using a conductor with a diameter of 34 mm. The optical head was attached to the conductor using adhesive tape. The most important properties of the sensor are its sensitivity of linearity to current and temperature dependency. Different current values were injected into the conductor using a DC supply device. For each current value, six samples were prepared, and the arithmetic mean was used. The device-generated current values ranging between 0A and 220A were connected in series to the conductor. Dedicated consideration was taken to place the sensor far enough from the current device to reduce the frequency interference. The current sensor response signals were acquired using a photodiode which converts the optical signal to an electric current intensity.

The influences of temperature dependency were carried out. The output signal for the sensor was measured at different temperatures using a thermometer and a big solenoid. The sensor head, along with the thermometer, was placed in the center but away from the inner wall of the solenoid. The output signal was measured from $T = 10\text{ }^{\circ}\text{C}$ to $T = 70\text{ }^{\circ}\text{C}$ at the same intensity of the magnetic field. The stability of the system was tested at different periods, keeping all conditions the same, including the temperature, etc. In addition, an isolated system is designed to ensure that the experimental setup is insulated from the external environment. The whole test bench is wrapped in a 30mm thick black rubber plastic material to achieve the purpose of heat insulation.

III. RESULTS AND DISCUSSION

A. Sensing Head Based on Light Transition

The experimental device designed based on the optical transition of MOCT is shown in Fig. 2. It consists of two linear polarizers, magneto-optical glass, conductor, laser, and photodiode detector. The schematic diagram of this experimental device is shown in Fig. 3.

The Faraday rotation angle β can be calculated using the output light intensity difference with field /without the field in (3) to (5) [15], where I_{trans} is the output laser power after the light goes through the sample without field, I_{field} is the output laser power with the field, ΔI_{nt} is the difference between I_{trans} and I_{field} , β is the Faraday rotation angle with the field. So, the difference of current ΔI_{nt} can be figured out using:

$$I_{field} = I_{trans} \cos^2(\alpha + \beta) \quad (3)$$

$$\Delta I_{nt} = I_{trans} - I_{field} \quad (4)$$

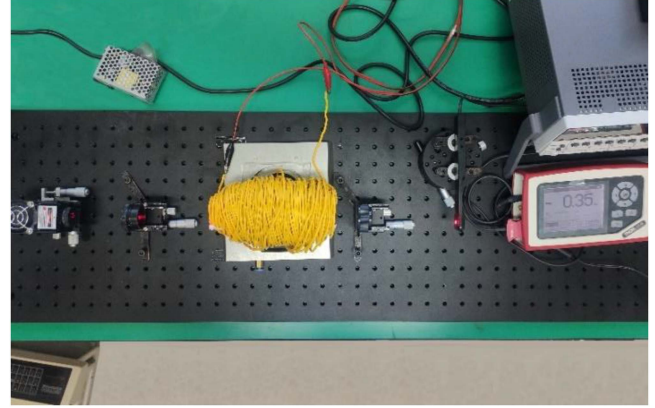


Fig. 2. Real setup for the designed current sensor based on the light transition.

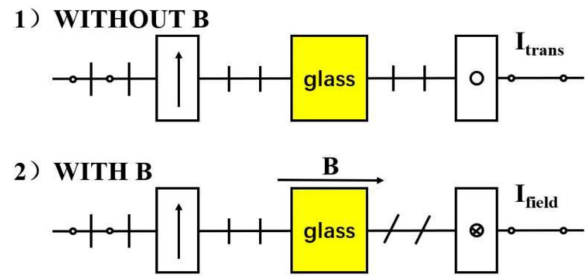


Fig. 3. Single light beam passing through the glass with or without the applied field B.

Typically, the polarizer and analyzer are arranged at an angle α of 45° . With no applied field, the optical power input to the photodiode is only half the input power. If the rotation angle β is not very big, the change in detector output is practically a linear function of the field. From (3), where α is replaced by $45^{\circ} + \beta$, the optical power at the detector is given by:

$$\Delta I_{nt} = I_{trans} \sin^2(\beta) \propto I_{trans} \beta^2 \quad (5)$$

The Verdet constant of the TPZBF sensing head was calculated to be $0.2 \text{ min}/(\text{G}\cdot\text{cm})$ at 632.8 nm , nearly 15 times higher than that of the silica glass ($V_{silica} = 0.01352 \text{ min}/(\text{G}\cdot\text{cm})$), which ensures an increased sensitivity of the sensor at low cost [12]. This glass does not suffer from problems such as temperature compensation, intrinsic birefringence, and bending-induced linear birefringence that usually occur in optical fiber sensing elements.

The I_{trans} , I_{field} , and ΔI_{nt} under 220A current in the optical transition model are shown in Table II. The length of the head was 40 mm.

According to (3) to (5), the Faraday rotation angle with the field can be calculated.

$$\beta = \sqrt{\frac{\Delta I_{nt}}{I_{trans}}} = \sqrt{\frac{1.202 \mu\text{w}}{7.445 \mu\text{w}}} = 23 \text{ degree}$$

This accuracy D can be expressed as a function of the difference between the I_{max} and I_{ave} divided by the I_{ave} , the functional

TABLE II
THE I_{trans} , I_{field} AND ΔI_{nt} IN THE OPTICAL TRANSITION MODEL

Samples number	I_{trans} (μW)	I_{field} (μW)	ΔI_{nt} (μW)
1	7.445	6.244	1.201
2	7.445	6.243	1.202
3	7.441	6.240	1.201
4	7.449	6.245	1.204
5	7.441	6.239	1.202
6	7.449	6.247	1.202

According (3) to (5), the Faraday rotation angle with the field can be calculated.

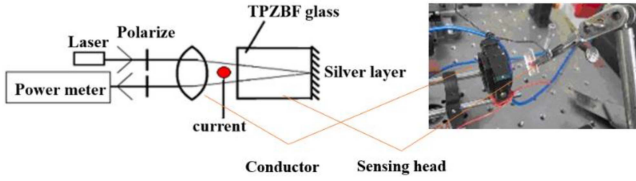


Fig. 4. Schematically/real setup for the designed current sensor based on light reflection.

relationships are shown in (6).

$$D = \frac{I_{max} - I_{ave}}{I_{ave}} \times 100\% \quad (6)$$

Accuracy is the difference between the average value and the truth value of the data in each independent measurement, and it is used to indicate the magnitude of the error. So, the measurement of the sensor accuracy is significant. According to (6), the accuracy of I_{trans} and I_{field} are respectively 0.067% and 0.064%, and the sensor accuracy is less than 1/1000. It can be proved that the values measured by the sensor are accurate, and the application of the optical current sensor is reliable.

B. Design of Sensing Head Based on Light Reflection

Another prototype of MOCT based on TPZBF glass with a sputtered silver layer that acts as a mirror to reflect the light is shown in Fig. 4. In this design, the light path in TPZBF glass was doubled.

The laser passed through the polariser and became linearly polarised light. The convex surface focused the light on the silver film of the TPZBF glass, which was placed in a current-induced magnetic field. The reflex light passes through the convex again and through the analyzer and was detected by the power meter. The input signal was a laser, and the output signal was a voltage. Fig. 5 shows the schematic cross-section of a wire and magnetic field, where $I = 220A$, $x_1 = 10$ mm, $x_2 = 2.5$ mm.

Theoretical and experimental magnetic field distributions are shown in Fig. 6. As can be seen, the uniformity of the magnetic field strength inside the electromagnetic coil is consistent with the direction, and the magnetic field strength is weak when far from the center of the solenoid coil, the closer it gets to the center of the solenoid, the more concentrated the size distribution of the magnetic field. The sample was positioned at the center of the solenoid, where a magnetic flux density value $B = 1.2mT$.

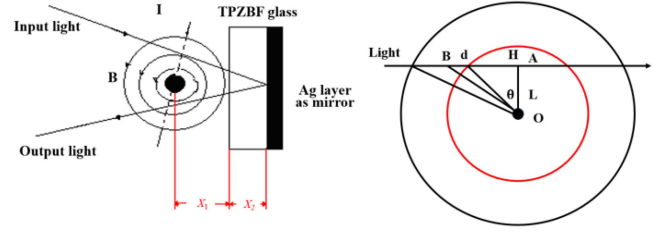


Fig. 5. Schematic cross-section of a current wire, $I = 220A$, $L = 15$ mm, $H = 40$ mm.

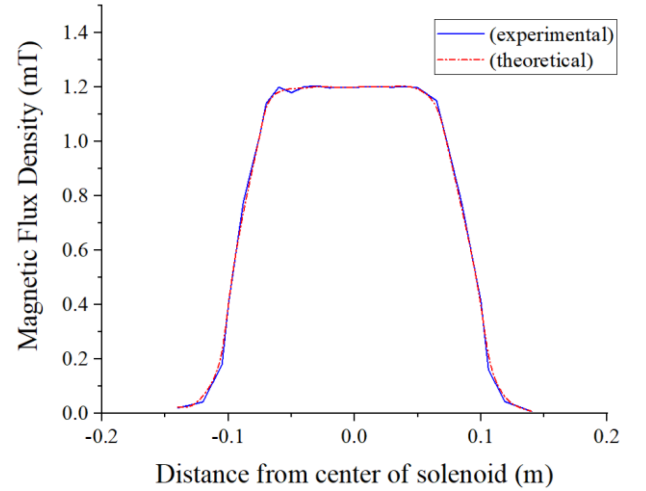


Fig. 6. Magnetic field density with respect to position along the solenoid.

The rectangular-shaped TPZBF glass sensing element with the deposited Ag layer was well polished with two side faces. Assuming the shortest distance between the current wire and light is L , the length of the glass is H and the thickness of the glass is d , the circular magnetic field in an infinite wire can be calculated for any point along the circular of the conductor using the following formula [17]:

$$B = \frac{\mu_0 I}{2\pi R} \quad (7)$$

Where the R is the distance from the wire axis, the constant μ_0 coefficient is $\mu_0 = 1.26 \times 10^{-6} \text{ B}\cdot\text{m}^{-1}$ and I is the current of the wire.

$$R = \frac{L}{\cos \theta} \quad (8)$$

So, the Faraday rotation angle β in the magnetic field can be defined as:

$$\beta = BvdL = \frac{\mu_0 I v}{2\pi R} \cos \theta dH \quad (9)$$

Where the dH is integral along the light path,

$$dH = \frac{L}{\cos \theta} d\theta \quad (10)$$

So, the Faraday rotation angle β can be figured out through (7) to (10) in the experiment.

In the prototype based on the light reflection, using (1), (7), and (10), when the applied current $I = 220A$, the Faraday angular

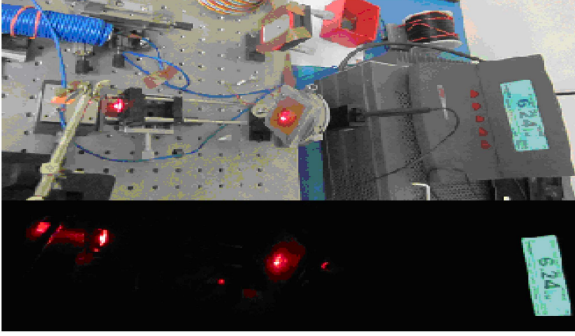


Fig. 7. Test of the output light stability at different time periods under the same conditions.

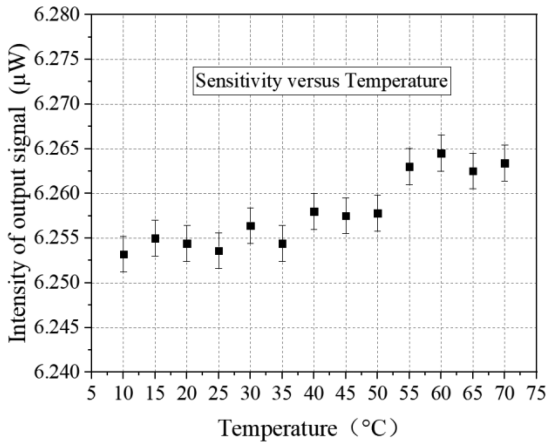


Fig. 8. Response from MOCT at different temperatures.

is 32 degree; this increased rotation angle is attributed to the increase of light passing through the length of the glass and the polarised light that is rotated twice in the same TPZBF glass. This design's sensitivity is the two values are very close to each other, which proved that the constructed system is accurate. In order to evaluate the stability of the system, a test on sensor elements versus different periods was performed under the same conditions. The schematic diagram of the calibration measurement device is shown in Fig. 7. The upper image was obtained at day, and the below one was obtained after 48 hours at night. The values of the light density through the photodiode did not change. This means that the device is stable, and the influence of external factors, such as the noise from the received optical signal and the noise floor of the system can be ignored.

The influence of temperature on sensitivity is reported in Fig. 8. Even though the sensor did not exhibit a strictly linear relationship between temperature and output intensity, the intensity changes under different temperatures were minimal. The intensity of the output signal varied between 6.25 and 6.26 μW , and the maximal temperature drift for the TPZBF sensor head was about $\Delta I_{nt} = 0.0124\text{nW}$ (for $T = 10^\circ\text{C}$ to 70°C), which means that minor variances in temperature cannot result in a significant intensity change.

The sensitivity versus different temperature should be $2.06 \times 10\text{nW}/^\circ\text{C}$ under the temperature ranging (10°C – 70°C).

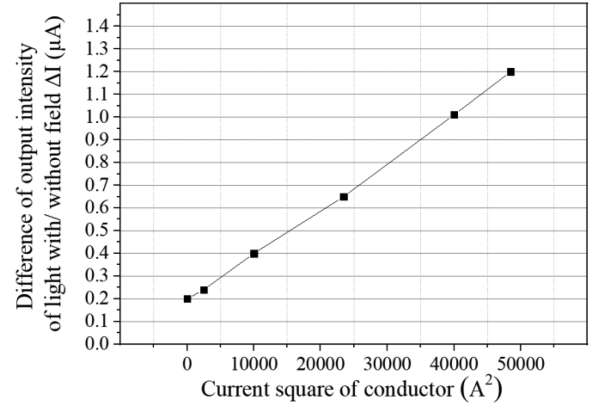


Fig. 9. Response of the sensor outputs as a function of the applied current square.

In order to determine the sensitivity to current, we plotted the $B^2 \sim \Delta I_{nt}$ curves for high magnetic fields. The magnetic field was generated by a direct current ($I_{max} = 220\text{A}$) on a conductor wire with a solenoid supplied by a DC source. Using the relations of I , B , ΔI_{nt} , and β , it can be considered that $I^2 \sim B^2 \sim \beta^2 \sim \Delta I_{nt}$. Fig. 9 shows the relation between the I^2 and ΔI_{nt} .

From this figure, as expected, it is clear that the response of the current sensor ΔI_{nt} is highly linear with the applied current squared I^2 , which means that in a fixed system, the output of the signal difference ΔI_{nt} is only related to the applied current I . The result is also related to the previous tests on the rotation angle, and different cycles are relatively consistent. These results proved that this designed MOCT is a good sensor prototype for highly sensitive currents sensing applications. The sensitivity to different applied currents can be expressed as $\Delta I_{nt}/I^2$. Considering the difference of output that was caused by light way reconnection and re-setup for each time, the average sensitivity for the sensor is $0.03\text{nW}/\text{A}^2$. In practice, the sensitivity can be improved by reducing the excess loss from the optical head and the output current error because with the decrease of the applied current on the conductor, the Faraday rotation angle will continually decrease. It will increase the difficulty of the acquisition of correct outputs. This possibility can be eliminated using a higher resolution rotation stage to install on the analyzer. On the other hand, the nonlinear behavior at different temperatures is also attributed to the conductor wire heating under a high current like 220A, which caused uncertainty to the measured temperature. Finally, precaution was also taken for safety under high current operations using the solenoid by selecting the lowest resistance wire. Optimization of the test system was also performed by making a stable bench which is an isolated system far away from other high voltages and heat sources. Ensure that the experiment is carried out under a closed, black condition, excluding other interfering factors.

IV. CONCLUSION

The optical current sensor has been developed based on high Verdet constant diamagnetism glass using a single light way and double polarimetric processing scheme. The sensing principle, its visual design, as well as its characterization have been

described. The performance of the prototype was evaluated, and experimental results showed that the magneto-optical current sensing system is stable, sensitive to applied current changes, insensitive to temperature differences, and high accuracy; these properties ensure that it is a good candidate for high voltage system applications.

REFERENCES

- [1] Z. Y. Ou et al., "Self-biased magnetoelectric current sensor based on SrFe₁₂O₁₉/FeCuNbSiB/PZT composite," *Sensors Actuators A: Phys.*, vol. 290, no. 1, pp. 8–13, Mar. 2019, doi: [10.1016/j.sna.2019.03.008](https://doi.org/10.1016/j.sna.2019.03.008).
- [2] S. C. Wang, F. Wan, H. Zhao, W. G. Chen, W. C. Zhang, and Q. Zhou, "A sensitivity-enhanced fiber grating current sensor based on giant magnetostrictive material for large-current measurement," *Sensors*, vol. 19, no. 8, Apr. 2019, Art. no. 1755, doi: [10.3390/s19081755](https://doi.org/10.3390/s19081755).
- [3] J. D. Lopez et al., "Fiber-optic current sensor based on FBG and optimized magnetostrictive composite," *IEEE Photon. Technol. Lett.*, vol. 31, no. 24, pp. 1987–1990, Dec. 2019, doi: [10.1109/lpt.2019.2952255](https://doi.org/10.1109/lpt.2019.2952255).
- [4] X. J. Zhang, "The study of the polarization errors of all fiber optical current transformers," in *Proc. IOP Conf. Ser.: Mater. Sci. Eng.*, vol. 562, no. 1, 2019, Art. no. 012079, doi: [10.1088/1757-899x/562/1/012079](https://doi.org/10.1088/1757-899x/562/1/012079).
- [5] Y. Qian, Y. Zhao, Q. L. Wu, and Y. Yang, "Review of salinity measurement technology based on optical fiber sensor," *Sensors Actuators B: Chem.*, vol. 260, no. 1, pp. 86–105, 2018, doi: [10.1016/j.snb.2017.12.077](https://doi.org/10.1016/j.snb.2017.12.077).
- [6] Q. L. Chen, H. Wang, Q. W. Wang, and Q. P. Chen, "Properties of tellurite core/cladding glasses for magneto-optical fibers," *J. Non-Crystalline Solids*, vol. 400, no. 15, pp. 51–57, May 2014, doi: [10.1016/j.jnoncrysol.2014.05.001](https://doi.org/10.1016/j.jnoncrysol.2014.05.001).
- [7] S. Y. Yin et al., "Study on the optical properties of high refractive index TeO₂-PbO-ZnO-BaF₂ glass system," *Adv. Mater. Sci. Eng.*, vol. 2021, no. 8, pp. 1–9, 2021, doi: [10.1155/2021/6466344](https://doi.org/10.1155/2021/6466344).
- [8] L. Yu, W. P. Guo, M. Sun, and J. He, "Elliptical measurement for faraday rotation in multimode TeO₂-ZnO-Na₂CO₃ fiber for magneto optical current sensor application," *Adv. Mater. Res.*, vol. 785–786, pp. 1367–1373, 2013.
- [9] A. C. S. Brigida et al., "Experimental and theoretical analysis of an optical current sensor for high power systems," *Photon. Sensors*, vol. 3, no. 1, pp. 26–34, 2013, doi: [10.1007/s13320-012-0092-1](https://doi.org/10.1007/s13320-012-0092-1).
- [10] Y. N. Ning, B. C. B. Chu, and D. A. Jackson, "Interrogation of a conventional current transformer by a fiber-optic interferometer," *Opt. Lett.*, vol. 16, no. 18, pp. 1448–1450, 1991, doi: [10.1364/OL.16.001448](https://doi.org/10.1364/OL.16.001448).
- [11] O. Tonnesen, N. Beatty, and O. A. Skilbreid, "Electrooptic methods for measurement of small DC currents at high voltage level," *IEEE Power Eng. Rev.*, vol. 9, no. 7, pp. 41–42, Jul. 1989, doi: [10.1109/mper.1989.4310789](https://doi.org/10.1109/mper.1989.4310789).
- [12] C. N. Rao, P. Dua, P. Kuchhal, Y. Lu, S. N. Kale, and P. J. Ca, "Enhanced sensitivity of magneto-optical sensor using defect induced perovskite metal oxide nanomaterial," *J. Alloys Compounds*, vol. 797, no. 15, pp. 896–901, 2019, doi: [10.1016/j.jallcom.2019.05.118](https://doi.org/10.1016/j.jallcom.2019.05.118).
- [13] Z. M. Liu et al., "Study of the Verdet constant of the holmium-doped silica fiber," *OSA Continuum*, vol. 3, no. 5, pp. 1096–1104, 2020, doi: [10.1364/OSAC.390111](https://doi.org/10.1364/OSAC.390111).
- [14] J. Zubia, L. Casado, G. Aldabaldetrekua, A. Montero, E. Zubia, and G. Durana, "Design and development of a low-cost optical current sensor," *Sensors*, vol. 13, no. 10, pp. 13584–13595, 2013, doi: [10.3390/s131013584](https://doi.org/10.3390/s131013584).
- [15] Q. L. Chen, H. Wang, Q. W. Wang, and Q. P. Chen, "Faraday rotation influence factors in tellurite-based glass and fibers," *Appl. Phys. A*, vol. 120, no. 3, pp. 1001–1010, 2015, doi: [10.1007/s00339-015-9268-z](https://doi.org/10.1007/s00339-015-9268-z).
- [16] S. Y. Yin et al., "Analysis of Faraday effect in multimode tellurite glass optical fiber for magneto-optical sensing and monitoring applications," *Appl. Opt.*, vol. 51, no. 19, pp. 4542–4546, 2012, doi: [10.1364/AO.51.004542](https://doi.org/10.1364/AO.51.004542).
- [17] Q. L. Chen, Q. W. Wang, H. Wang, and Q. P. Chen, "Structural and properties of heavy metal oxide Faraday glass for optical current transducer," *J. Non-Crystalline Solids*, vol. 429, no. 1, pp. 13–19, 2015, doi: [10.1016/j.jnoncrysol.2015.08.031](https://doi.org/10.1016/j.jnoncrysol.2015.08.031).